Aeolian Research 20 (2016) 25–33

Contents lists available at ScienceDirect

Aeolian Research

journal homepage: www.elsevier.com/locate/aeolia

Quantitative modeling of facet development in ventifacts by sand abrasion

Péter L. Várkonyi [a,*], Julie E. Laity [b], Gábor Domokos [a]

[a] Department of Mechanics, Materials and Structures, Budapest University of Technology, Műegyetem rkp. 3, H-1111 Budapest, Hungary
[b] Department of Geography, California State University, Northridge, 18111 Nordhoff Street, Northridge, CA 91330-8249, USA

ARTICLE INFO

Article history:
Received 23 April 2015
Revised 21 October 2015
Accepted 21 October 2015
Available online 21 November 2015

Keywords:
Ventifacts
Morphology
Abrasion
Facet
Quantitative modeling
Wind abrasion

ABSTRACT

We use a quantitative model to examine rock abrasion by direct impacts of sand grains. Two distinct mechanisms are uncovered (unidirectional and isotropic), which contribute to the macro-scale morphological characters (sharp edges and flat facets) of ventifacts. It is found that facet formation under conditions of a unidirectional wind relies on certain mechanical properties of the rock material, and we confirm the dominant role of this mechanism in the formation of large ventifacts. Nevertheless small ventifacts may also be shaped to polyhedral shapes in a different way (isotropic mechanism), which is not sensitive to wind characteristics nor to rock material properties. The latter mechanism leads to several 'mature' shapes, which are surprisingly analogous to the morphologies of typical small ventifacts. Our model is also able to explain certain quantitative laboratory and field observations, including quick decay of facet angles of ventifacts followed by stabilization in the range 20–30°.

1. Introduction

For more than 150 years, the shapes of wind-worn rocks (ventifacts), including facets and sharp edges, have inspired researchers to describe the underlying abrasion mechanism (Blake, 1855). The abundance of such formations on Mars has renewed interest in this topic.

Ventifact research in the late 19th (Enys, 1878; Stone, 1886; and others) and early 20th centuries (Bather, 1900; Bryan, 1931; King, 1936) concentrated in large measure on the morphological classification and documentation of small ventifacts. While there is no precise definition of a 'small' ventifact, it is generally considered to be a few centimeters in diameter (Schoewe, 1932; Wentworth and Dickey, 1935; Needham, 1937), whereas 'large' ventifacts may reach heights of several meters (Laity, 2009). Bather (1900) referred to small wind-eroded rocks as dreikanter, pyramid-pebbles, or facetted pebbles and, in 1911, Evans proposed that the term 'ventifact' be employed to encompass the multiple terms then in use. For small rocks in particular, the original faces of a rock are modified by wind abrasion to form one or more facets – approximately planar rock surfaces (Bather, 1900; King, 1936; Sharp, 1949), with a keel (sharp ridge) or keels joining two or more facets. Early ventifact studies devoted considerable energy to classification and the number of keels (kante) was used to describe small ventifacts as einkante, zweikanter, dreikanter (one-, two-, three-ridged), etc. (Bryan, 1931).

The relationship between ventifact form, wind climate, and the nature of the abradant has been a longstanding area of inquiry. Throughout the early period of investigation, debates centered on whether facets were caused by unidirectional winds, by winds from two opposing directions, or winds from multiple directions (termed here: variable winds). Additionally, the degree to which the shapes of mature ventifacts reflect the initial clast morphology or the wind direction was considered (see, for example, Wade, 1910; King, 1936; Sugden, 1964). In an extensive review of earlier investigations into faceted pebbles, Bather (1900) concluded that (a) facets, polish, and striations are the result of wind-blown sand and (b) that facets form by the action of the prevailing winds, with the wind acting at right angles to ridges (keels). More recent research supports these fundamental findings (Laity and Bridges, 2009). Today, it is widely accepted that ventifact morphology reflects the local, and in some cases, regional, wind direction and large ventifacts have been used as indicators of palaeoclimate and palaeowinds, both on Earth and Mars (Laity, 1987; Bridges et al., 1999, 2014; Thomson et al., 2008).

The development of individual facets has received considerable qualitative consideration over the duration of ventifact studies. It is an established view that every facet of a clast corresponds to a

* Corresponding author. Tel.: +36 20 251 0668.
E-mail addresses: vpeter@mit.bme.hu (P.L. Várkonyi), julie.laity@csun.edu (J.E. Laity), domokos@iit.bme.hu (G. Domokos).

http://dx.doi.org/10.1016/j.aeolia.2015.10.006
1875-9637/

sustained period of immobility during the abrasional history, associated with a constant dominant wind direction relative to the rock. The principal questions that have been posed are the effect of the original shape of the rock face on facet development and the causes of multiple facets. With respect to small ventifacts, studies as early as Bather (1900) suggest that facet morphology reflects the shape of the original clast, especially in the early stages of abrasion. Field observations show that medium- to large-sized boulders typically have one or two facets or beveled faces reflecting the dominant wind directions; whereas, smaller ventifacts often acquire several facets as they are more easily displaced and a new facet will form with each movement (Woodworth, 1894; Cooke et al., 1993; Hoare et al., 2002). Causes of rock displacement include animal disturbance, frost shifting, undermining by rainwash or the wind, and earthquakes. Furthermore, King (1936) suggests that attrition of the rock by sandblasting from two directions may produce a narrow base, which causes the stone to roll over, providing a fresh face on which new facets are cut. These conditions apply where the ventifact is not firmly anchored in the substrate, but is free to move.

In addition to facets and edges, wind direction is reflected in meso-scale surface patterns, such as flutes, grooves, and pits. The morphological evolution of these features and the time required for their formation remain an area of ongoing investigation (Knight and Burningham, 2003; Bridges et al., 2004; Várkonyi and Laity, 2012). Understanding such feature evolution provides important clues to the age and maturity of a wind-eroded landscape (Knight, 2008; Gillies et al., 2009; Bridges et al., 2014). A long-lasting debate in the literature has focused on the relative importance of saltated sand grains vs. suspended dust particles in the formation of surface features (Laity and Bridges, 2009). Today, it is widely accepted that sand dominates abrasion – the present work also adopts this view. In a recent paper (Várkonyi and Laity, 2012), we developed a differential equation model of abrasion to demonstrate that abrasion by direct impacts from sand grains is able to develop, maintain and enlarge various meso-scale features such as pits, flutes and grooves.

Only a few attempts have been made to develop quantitative models of abrasion and study how the evolving rock geometry and the abrasion process interact with each other (Anderson, 1986; Wang et al., 2011; Várkonyi and Laity, 2012; Barchyn and Hugenholtz, 2015). Facet evolution has been shown to proceed by sand abrasion of targets under both laboratory (Kuenen, 1928,1960) and field conditions (Bridges et al., 2004). The facets developed on large ventifacts may be transitional in form to those developed on the lower windward faces of yardangs, which evolve in a similar manner, but are embedded, and thus not subject to movement. Kuenen's (1928) laboratory experiments suggested that the eventual form of the ventifact (ridge-shaped or pyramidal, for example) is determined by the initial shape of the base, but the experimental conditions did not allow undermining of the base and subsequent reorientation of the faces. Schoewe (1932) simulated conditions of overturning and examined both unidirectional and variable winds (from 16 directions) and noted the development of similar end forms, with the triquetous or Brazil-nut type considered to be the final or most complete shape. The triquetous and tetrahedron forms (Woodworth, 1894; Bather, 1900) (see Fig. 1) are thought to represent a shape attained by "completed" aeolian action under field conditions (Enys, 1878). In addition to form experiments, there are some data on the abrasion rate under various conditions (Selby, 1977; Sharp, 1980; Miotke, 1982; Greeley et al., 1985; Malin, 1988; Knight, 2003; Knight and Burningham, 2003). Under conditions of abundant sediment and persistent winds, the initial form of ventifacts can develop quickly. However, ventifact form is controlled by the highest velocity winds in a region, which are infrequent. Thus, mature ventifact forms may take a centuries or millennia to develop (Anderson and Anderson, 2010).

Our present goal is to develop a model of abrasion suitable for numerical simulation, which illustrates the formation of ventifact macro-scale edges (keels) and facets, and which predicts the shapes of mature ventifacts. We analyze the formation of facets on both large and small ventifacts. Large specimens are usually immobile, and the strongest winds around them very often have one dominant direction. We demonstrate that the resulting abrasion mechanism (which we will call henceforth *unidirectional mechanism*) rapidly generates facets and edges due to the special dependence of the abrasion susceptibility of rock material to impact angle.

In order to understand the morphological evolution of small ventifacts, we analyze a simplified model of the abrasion of a specimen that is small enough to get overturned many times. Given the frequent causes of displacement discussed earlier, it is perhaps unlikely to rest long enough in one position to acquire well-defined facets. Our model reveals that this scenario can be modeled as a continuously varying wind direction relative to the rock, leading to uniform abrasion over the rock surface. This process induces facet and edge formation through a different mechanism than the unidirectional mechanism, which we refer to as the *isotropic mechanism*. Facet formation via the isotropic mechanism is somewhat less efficient than facet formation via the unidirectional mechanism. At the same time, it is effective on all material types, as it does not rely on a special dependence of susceptibility to impact angle. To judge the practical significance of the isotropic mechanism, future work is needed to compare the frequency of rock displacements to the time-scale of abrasion.

The newly uncovered isotropic mechanism transforms any initial shape to one of three 'ultimate' shapes, two of which resemble the most common mature ventifact morphologies: pyramidal dreikanters and triquetrous Brazil nut shapes (Fig. 1). Which of these alternatives emerges depends only on the geometry of the initial shape as explained in Section 3.2.

In this paper we extend aspects of the methodology in Várkonyi and Laity (2012), including numerical simulation of ventifact development using different rock materials. The model subjects the rock to both unidirectional and variable winds, the latter representing the action of wind on a frequently displaced rock. In all cases, it is assumed that the material is homogeneous and without cavities. This differs from our previous work, where we examined the growth of linear features, such as flutes, on large, inhomogeneous rocks with cavities that, owing to their mass, were fixed in position (Várkonyi and Laity, 2012).

2. The abrasion model

Várkonyi and Laity (2012) proposed a partial differential equation as a model of abrasion. Here we briefly summarize the model.

2.1. Energy flux of impactors

Let the position vector **x** point to a surface point of an abrading rock. The area around this surface point experiences impacts from sand grains of various impact angles (φ). Throughout the paper, φ is defined as the angle between the particle's trajectory and the tangent plane of the rock surface (i.e., $\varphi = 0$ for grazing impacts, and $\varphi = 90°$ for perpendicular impacts). The long-term statistical distribution and the intensity of impacts can be characterized by a mean energy flux distribution function $F(\varphi,\mathbf{x})$ with dimension mass^1 time^{-3}. The integration of this function over areas of the rock surface, and ranges of φ, provides the total kinetic energy of impactors hitting the examined area per unit time, within the

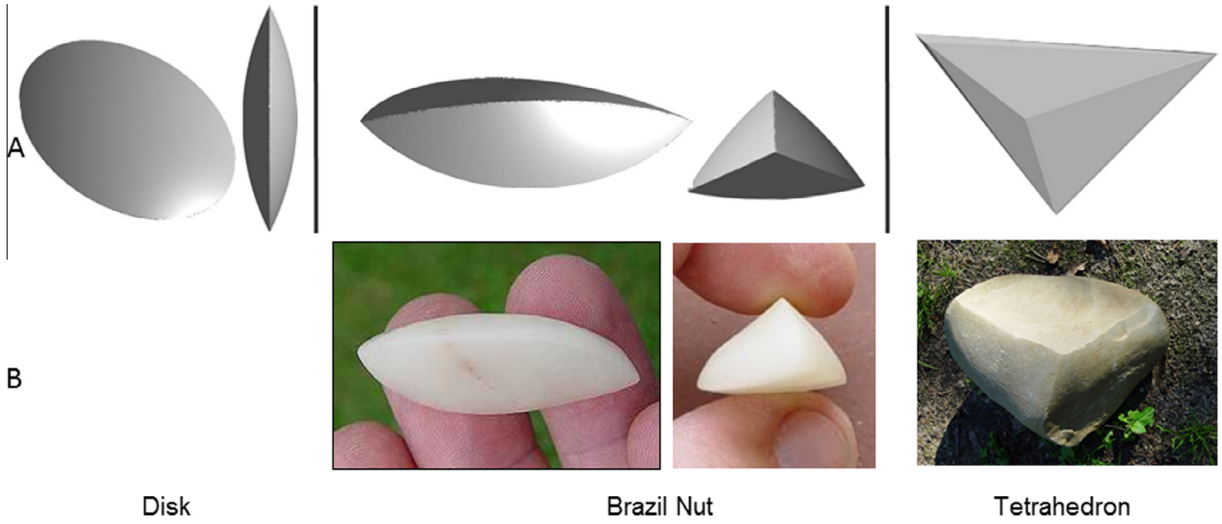

Fig. 1. (A) The three mature shapes of small ventifacts predicted by the model described in this paper. Two views of flat disk with two curvilinear facets and an edge (left); two views (long axis and end view) of an elongated 'Brazil nut' shape with three curvilinear facets and three edges (middle); one view of an arbitrarily shaped tetrahedron (right). (B) Photos of actual ventifacts: small ventifact from the Libyan desert (middle); and periglacial ventifact from Germany (right). Flat disk-shaped ventifacts appear to be uncommon in the field. Photos by Matthias Bräunlich.

given ranges of φ. There are theoretical and empirical results on how the *instantaneous* energy flux for surfaces facing the wind depends on wind velocity and height above ground (Bridges et al., 2005; Anderson and Anderson, 2010). Other important factors to be considered include the orientation of the surface of the rock relative to the ground surface and to the instantaneous wind direction; as well as the availability of sand. To find the long-term distribution $F(\varphi,\mathbf{x})$, the wind regime of a given location, as well as displacements in the case of mobile rock specimens should also be considered. Simple examples of finding $F(\varphi,\mathbf{x})$ are given in Section 2.3.

2.2. Abrasion susceptibility of rock material

The rate of abrasion of a rock surface is known to be linearly proportional to the total kinetic energy flux of impactors hitting it (Greeley et al., 1985). A recent work (Wang et al., 2011) has also uncovered the dependence of abrasion rate on mechanical properties of the rock, including Young's modulus and shear strength. Finally, the impact angle of the sand particles plays a key role in abrasion (Greeley et al., 1985). In line with these results, the abrasion effect of the impacts is characterized by a susceptibility function S defined as the volume of the eroded material per unit kinetic energy of the impacting grains (dimension: length^1 mass^{-1} time^2). S is assumed to take the form $S = Cs(\varphi)$, where C has the same dimension as S. C is independent of impact angle, but it may depend on other factors such as mechanical properties of the rock material, whereas the dimensionless function $s(\varphi)$ incorporates the effect of impact angle. Throughout the rest of the paper, $s(\varphi)$ is referred to as the susceptibility function.

Rocks are usually considered as brittle materials, for which theoretical models suggest $s(\varphi) = \text{constant} \times \sin^2(\varphi)$ (Finnie, 1995, Fig. 2). Because of $S = Cs(\varphi)$, the constant multiplicator in the formula of $s(\varphi)$ can be chosen arbitrarily and thus the vertical axis of Fig. 2 is not scaled. Ductile materials (e.g., metals) have a significantly different susceptibility function due to the different mechanisms of abrasion (Fig. 2). Experiments on obsidian by Greeley et al. (1982, 1985) showed brittle behavior. However, they also found that many igneous rocks, including basalt, granite, tuff and rhyolite, behave as a 'combination of brittle and ductile material'. The behavior of these rocks is best described by an intermediate susceptibility function, which lies between the brittle and ductile types and has two susceptibility peaks: we refer to this curve as a 'Modelled susceptibility function' (Fig. 2) (Greeley et al., 1982, 1985). Non-igneous lithologies have not been examined experimentally. It is beyond the scope of this paper to clarify the contradiction between Greeley's experimental results and the fact that rock is usually considered brittle. Our results are discussed for Modelled and brittle material.

2.3. Abrasion equation

With the notations introduced above, the long-term mean rate of abrasion of the rock surface at point $\mathbf{x}$ is

$$\dot{\mathbf{x}} = \int_{\varphi=0}^{\pi/2} \underbrace{F(\varphi,\mathbf{x})}_{\substack{\text{distribution}\\ \text{of impacts}}} \cdot \underbrace{C \cdot s(\varphi)}_{\substack{\text{efficiency}\\ \text{of impacts}}} d\varphi \cdot \mathbf{n}(\mathbf{x}) \tag{1}$$

where $\mathbf{n}(\mathbf{x})$ is the inward pointing unit normal vector of the surface at $\mathbf{x}$. C is independent of φ, thus it can be moved outside the integral to obtain

$$\dot{\mathbf{x}} = C \cdot \int_{\varphi=0}^{\pi/2} F(\varphi,\mathbf{x}) s(\varphi) d\varphi \cdot \mathbf{n}(\mathbf{x}) \tag{2}$$

If $s(\varphi)$ and $F(\varphi,\mathbf{x})$ are known, this equation can be used to simulate the morphological changes of the retreating rock surface, which is the aim of this paper. C determines the time scale of the abrasion process, which is less important for our present purpose.

To estimate $F(\varphi,\mathbf{x})$ without a detailed analysis of saltation trajectories and impact events, we use two assumptions:

1. The impactors are much smaller than the rock surface under abrasion.
2. The trajectory of each grain follows the actual wind direction represented by a horizontal unit vector $\mathbf{w}$.

Assumption 1 is important, because impacts from large objects tend to accumulate at strongly curved portions of a rock surface, fundamentally changing the abrasion process (Várkonyi and Domokos, 2011). Assumption 2 neglects the fact that saltating sand grains have slightly curved trajectories, some parts of which deviate significantly from the horizontal. Assumption 2 also neglects

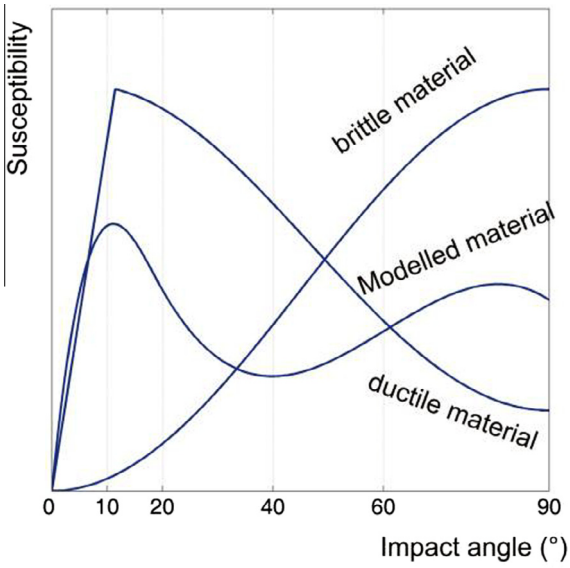

Fig. 2. Shape of the susceptibility function of an ideally brittle material; an ideally ductile material; and a schematic curve based on Greeley's (1982) experiments on the susceptibility of various volcanic rocks, labeled as 'Modelled material'.

impactor deviation in the neighborhood of a rock caused by local perturbations of the airflow, which is realistic because coarse grains, transported by saltation, tend to decouple from the wind flow (Anderson, 1986).

While the modeling framework presented in this paper can be used to simulate arbitrary wind conditions, in the following we narrow our focus to three idealized scenarios:

Unidirectional wind: Aeolian abrasion is maximized during episodes of strong winds, wherein the direction tends to show little fluctuation. To study facet formation in the presence of a unidirectional wind, we assume that all grains move in the same direction ($\mathbf{w}$) and their flux is independent of $\mathbf{x}$. Then, all impacts hitting at a given point have the same impact angle, namely 90° minus the angle between $\mathbf{n}(\mathbf{x})$ and $\mathbf{w}$. This angle is denoted by $\beta(\mathbf{x})$. The distribution function F can be expressed using the Dirac-delta (Δ) symbol: $F(\varphi,\mathbf{x}) = \text{constant}\cdot E(\mathbf{x})\max(0,\sin\beta(\mathbf{x}))\cdot\Delta(\varphi-\beta(\mathbf{x}))$. $E(\mathbf{x})$ is an exposure function: it is 1 on portions of the surface exposed to the grain flux and 0 for sheltered parts. The sheltered parts include all leeward surfaces ($\sin\beta(\mathbf{x}) < 0$) and they may include some parts of windward surfaces, which are shadowed by other portions of the rock surface. We restrict our attention to convex shapes, on which windward areas are always exposed to abraders. In this case, the abrasion Eq. (2) becomes

$$\dot{\mathbf{x}} = \text{constant}\cdot\max(0,\sin\beta(\mathbf{x}))\cdot s(\beta(\mathbf{x}))\cdot\mathbf{n}(\mathbf{x}) \tag{3}$$

The same equation has been examined in Várkonyi and Laity (2012); however, the focus of that paper was on the effect of grains rebounding within cavities of a textured rock surface. In the present paper, we discuss smooth surfaces without cavities.

Variable wind: As discussed above, the direction of strong winds, which activate aeolian abrasion, usually does not fluctuate greatly. Nevertheless, small rocks may occasionally be displaced during the decade- or even century-long abrasion process. Each such event changes the apparent direction of the wind relative to the rock. Our goal is to model this scenario. If a rock is displaced many times during the abrasion process, the variable wind directions (relative to the rock) can be approximated by a continuous probability distribution. For the sake of simplicity, we assume that this distribution is uniform, i.e., that the stone rests in all orientations with equal probability. Under such conditions, a surface point on a simple, convex rock surface experiences impacts over time from all directions. F can be determined as an integral over a half-sphere (i.e., the horizon of the examined surface point). Provided that the grain flux is again independent of $\mathbf{x}$, $F(\varphi,\mathbf{x}) = \text{constant}\times\cos(\varphi)\cdot\sin(\varphi)$ and (Bloore, 1997; Várkonyi and Domokos, 2011). Hence, in this case, the intensity of abrasion is uniform over the rock surface for any material and any convex geometry. Concave parts of a rock are partially shadowed by other regions of the rock surface. The model is not extended to this case.

$$\begin{aligned}\dot{\mathbf{x}} &= \text{constant}\cdot\int_{\varphi=0}^{\pi/2}\cos\varphi\sin\varphi\cdot s(\varphi)d\varphi\cdot\mathbf{n}(\mathbf{x})\\ &= \text{constant}\cdot\mathbf{n}(\mathbf{x})\end{aligned} \tag{4}$$

Unidirectional wind with height-dependent intensity: The model can be made more realistic by taking into account that the intensity of the abrasion depends on the height $h(\mathbf{x})$ above the ground. Specifically, it is close to 0 at the ground level, increases with height up to a maximum point, and decreases to 0 again if height is further increased (Anderson, 1986). For small rocks, the intensity is roughly proportional to $h(\mathbf{x})$. The corresponding abrasion equation reads

$$\dot{\mathbf{x}} = \text{constant}\cdot\max(0,\sin\beta(\mathbf{x}))\cdot s(\beta(\mathbf{x}))h(\mathbf{x})\cdot\mathbf{n}(\mathbf{x}) \tag{5}$$

3. Simulation results

3.1. Facet formation in unidirectional wind

It is likely that the specific susceptibility function of brittle materials is responsible for the formation of facets facing towards the prevailing wind direction. This is confirmed and explained by the present model of abrasion. It can be shown that in the presence of unidirectional wind, the constant susceptibility function $s(\varphi)$ would result in a rock surface *retreating without changing its shape* (Fig. 3A). At the same time, a local peak in the susceptibility function at some angle φ_0 initiates accelerated abrasion in those areas of the rock, at which $\beta(\mathbf{x})$ is close to φ_0. The accelerated abrasion results in the *growth of areas* with $\beta(\mathbf{x})\approx\varphi_0$. Eventually, flat, windward-facing facets emerge if $\varphi_0 = 90°$ (Figs. 3B and 4B, C), and facets not perpendicular to the predominant wind direction are created for other values of φ_0 (Figs. 3C and 4C, D). Simultaneously, edges or vertices may form at the boundaries of quickly abrading faces.

The ideally brittle and the Modelled materials have peaks of sensitivity at $\varphi = 90°$, which explains why most ventifacts have facets directly facing the wind. In contrast, a ductile material is less sensitive to high-angle impacts than to impacts of intermediate angles. Thus, if a vertically standing cylinder is abraded, our abrasion model predicts the formation of a vertical edge facing towards the wind, surrounded by two quickly abrading flat areas. An example of this behavior is the butterfly wing-shaped abrasion pattern of a metal plate cover exposed to sand storms (Fig. 16 of Greeley et al., 2002). The susceptibility function of the Modelled material contains a second peak near $\varphi = 15°$. In such a case, the model predicts the formation of facets at oblique angles to the wind, but such occurrences have not been observed in the field. This may indicate that, contrary to the lab measurements of Greeley et al. (1982), rocks under field conditions behave more closely to an ideally brittle material.

To illustrate how efficiently abrasion creates polyhedral facets, we first develop a quantitative measure of "facetedness" of a geometrical shape. Recall first that the 'Gaussian curvature' at a point of a surface is defined as $\gamma = (r_1 r_2)^{-1}$ where r_1 and r_2 are the principal radii of curvature. It is a widely-known classical result of geometry that the integral of γ over the surface area of a solid without holes is always 4π (Hazewinkel, 2001). Hence, the average value

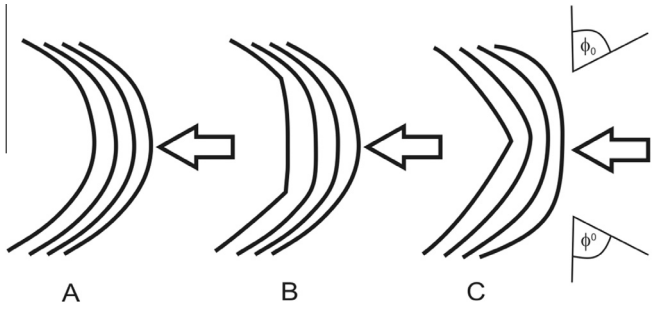

Fig. 3. (A) Planar illustration of the abrasion of a solid with angle-independent susceptibility in unidirectional wind: the rock surface retreats without changing its shape; (B) abrasion of a solid with maximum susceptibility at impact angle 90°; and (C) abrasion of a solid with a local peak in the susceptibility function at angle ϕ_0.

of γ is $4\pi/S$ where S is the total surface area. A portion of the rock surface can be considered as a flat face if γ is significantly lower over this portion than $4\pi/S$. This observation motivates the following 'measure of facetedness' (MF)

$$\mathrm{MF} = \frac{\text{surface area with } \gamma < 0.1 \times 4\pi/S}{S} \tag{6}$$

yielding a value between 0 (rounded shapes) and 1 (polyhedral shapes). To study the evolution of the MF, randomly rounded (but not exactly spherical) initial shapes have been generated by a simple computer algorithm and abraded according to the differential equation modeling unidirectional wind. The diagram of MF versus the remaining volume of the abraded shape is plotted both for 'brittle' and for Modelled material (Fig. 5). In both cases, the MF grows rapidly: specimens become significantly faceted after volume loss of a few percent.

3.2. Facet formation on frequently displaced rocks

Under the ideal conditions described in Section 2, the abrasion model predicts uniform abrasion over the surface of a rock being displaced many times during abrasion. It has been noted several times that uniform abrasion generates polyhedral shapes with a low number of facets (Schoewe, 1932; Kuenen, 1928, 1960). This is illustrated by a simple two-dimensional caricature in Fig. 6. Facet formation can be explained as follows: abrasion removes material gradually from the outside of a rock during abrasion. The lifetime of a piece of material within the abrading rock depends on how deep it is under the initial rock surface. Hence, the abrading rock shrinks to its deepest internal point. This point happens to be the center of the largest inscribed sphere of the original surface. The largest inscribed sphere touches the surface at 2, 3 or 4 points. (In degenerate cases, the number of points may exceed 4). The ultimate shape of an abrading rock depends on the number of touching points. If there are 4 points, the ultimate shape is a (not necessarily regular) tetrahedron with four facets, which preserves its shape in further abrasion; 3 points correspond to an elongated 'Brazil nut' shape with triangular cross-section, two tips, three edges and three curved faces; and 2 points to a flat disk shape with two smooth faces and a sharp, elliptic edge connecting them (Fig. 1A).

It is remarkable that two of the ultimate ventifact shapes predicted by the abrasion model show close similarity to the classification of mature ventifacts shapes. In particular, pyramidal

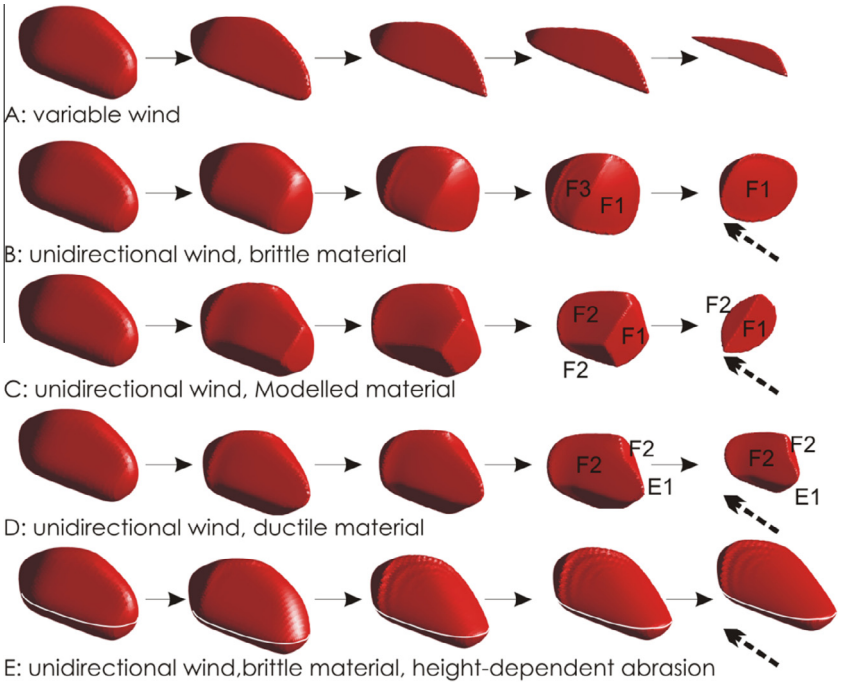

Fig. 4. Numerical simulation of the abrasion of a given shape under various conditions, using an open-access implementation of Level Set Methods in MatLab environment by Mitchell (2008). (A) variable wind is modeled by uniform abrasion. This process creates polyhedral shapes with positions of the faces determined by the initial clast morphology. For this example, the ultimate shape is an elongated 'Brazil nut' with 3 curved edges and 3 curvilinear facets (see Section 3.2) (B)–(D) abrasion due to unidirectional wind (Section 3.1). Wind direction denoted by dotted arrows. An ideally brittle material (B) develops a flat facet (F1) facing the wind. The Modelled material (C) develops a face perpendicular to the wind (F1) as well as other faces at an angle 10–20° to the wind (F2), reflecting the two peaks of the susceptibility function. A ductile material (D) exhibits an edge facing the wind (E1) and flat areas at angle 10–20° to the wind (F2). If the intensity of the abrasion is proportional to the height above the reference level marked by a white curve (E), brittle materials develop a windward facet, which becomes less and less steep. Notice that ventifact shapes are partly determined by the initial clast morphology, especially in early stages of abrasion: specifically, the large flattish area of the original clast initiates facet formation for all material types; nevertheless, this face disappears later for the brittle material (F3). The smooth initial shape was obtained by generating a random convex polyhedron and by smoothing it via numerical simulation of the mean curvature flow (non-uniform abrasion with rate linearly proportional to the mean curvature of the surface).

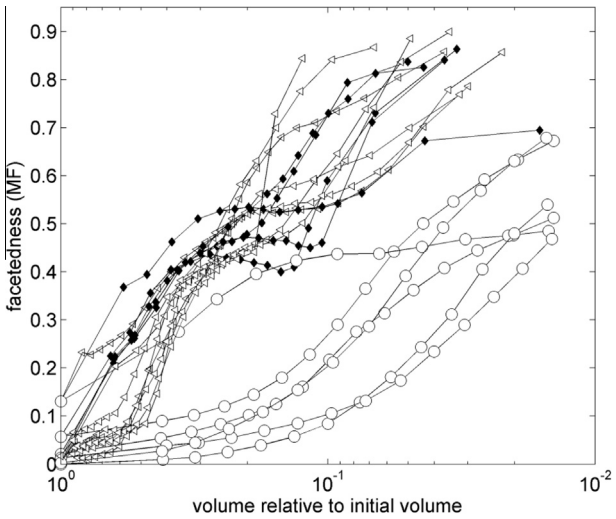

Fig. 5. Diagram of facetedness (MF) versus volume of the abraded rock relative to its initial value for seven random shapes. Empty triangles: brittle material in unidirectional wind. Filled diamonds: Modelled material in unidirectional wind. Circles: variable wind. The last curve does not depend on the shape of the susceptibility function of the specimen. The numerical solver, and the method of generating initial shapes are described in the caption of Fig. 4

Fig. 6. Planar illustration of ventifact formation by uniform abrasion. The distances between adjacent curves are constant. Typically, initially rounded objects develop flat facets at initially flatter portions, and sharp vertices where the initial shape is more curved. The object shrinks to the internal point furthest from its external surface, which is the center of the largest inscribed circle in 2D or sphere in 3D (dashed lines). The shape of the solid becomes polygonal with as many edges as the number of tangencies of the circle (in this case 3). Three dimensional objects similarly develop facets, edges and vertices. The number of facets of a worn shape are determined by the number of tangencies of the inscribed sphere in the initial state.

dreikanter ventifacts are closely related to tetrahedra, and "*...A common shape for small faceted ventifacts is a streamlined, almond or Brazil nut shape dominated by two or three surface facets...*" (Bourke and Viles, 2007). See Fig. 1B for some examples.

Flat disk-shaped ventifacts are uncommon. We suspect that this discrepancy of the model is caused by the failure of the basic modelling assumption that the stone rests in all orientations with roughly equal probability. Because its flatness, a disk-shaped ventifact would always rest on one of its flat sides. Thus, horizontally blowing winds would attack its sharp edge, destroying its morphological character.

The efficiency of the isotropic mechanism in creating facets has been tested and compared with the efficiency of the unidirectional mechanism (Fig. 5). The rate of increase of the MF value is somewhat lower than for unidirectional wind and thus the isotropic mechanism is less efficient in forming faceted ventifacts. At the same time, the isotropic mechanism creates the same shapes regardless of the susceptibility function of the material.

3.3. The decay of facet angles

It has been observed that the steepness of ventifact facets quickly decays to approximately 20–30°, as the abrasion progresses (Sharp, 1949; Laity and Bridges, 2009). At this point, the angle seems to stabilize. Decreasing angles have been explained by the height-dependent intensity of abrasion (implemented by Eq. (5)). Our goal is to demonstrate why the angle is stabilized at 20–30°. Let $\alpha(t)$ denote the time-dependent slope angle of a flat facet facing towards the wind. The surface of the facet is given in a d (horizontal) h (vertical) coordinate system by the equation $d(h,t) = h\cot\alpha(t)$. By (5), the abrasion rate is constant·$\sin\alpha(t)$·$s(\alpha(t))h$, which means that the surface moves in horizontal direction with velocity $\partial d(h,t)/\partial t = \text{constant} \times s(\alpha(t))h$. Thus, the time derivative of the facet angle is

$$\begin{aligned}\frac{d}{dt}\alpha(t) &= \frac{d}{dt}[a\tan(h/d(h,t))] = \frac{-h\cdot\partial d(h,t)/\partial t}{d^2(h,t)+h^2}\\ &= \text{constant}\times\frac{-s(\alpha(t))}{1+d^2(h,t)/h^2}\\ &= \text{constant}\times\frac{-s(\alpha(t))}{1+\cot^2(\alpha(t))}\end{aligned} \tag{7}$$

The evolution of the facet angle depends on the susceptibility function $s(\varphi)$. The $\alpha(t)$ curves given by the ordinary differential Eq. (7) are shown in Fig. 7 for ideally brittle and for Modelled materials. For brittle materials, α drops quickly to 20–30° and thereafter the rate of change becomes extremely low. In contrast, facet angles of the Modelled material continuously decay below 10°. Our results with brittle materials confirm field observations, whereas the angle at which facets on rocks with 'Modelled material' are stabilized contradicts field observations. This result strengthens the conclusion of Section 3.1 that rocks under terrestrial conditions behave as brittle rather than as Modelled materials. However, it contradicts to some extent Várkonyi and Laity (2012), where

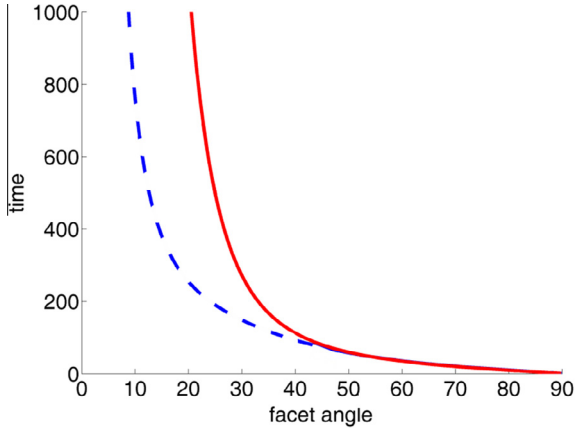

Fig. 7. Numerically simulated evolution of the facet angle for brittle material (continuous curve) and Modelled material (dashed curve).

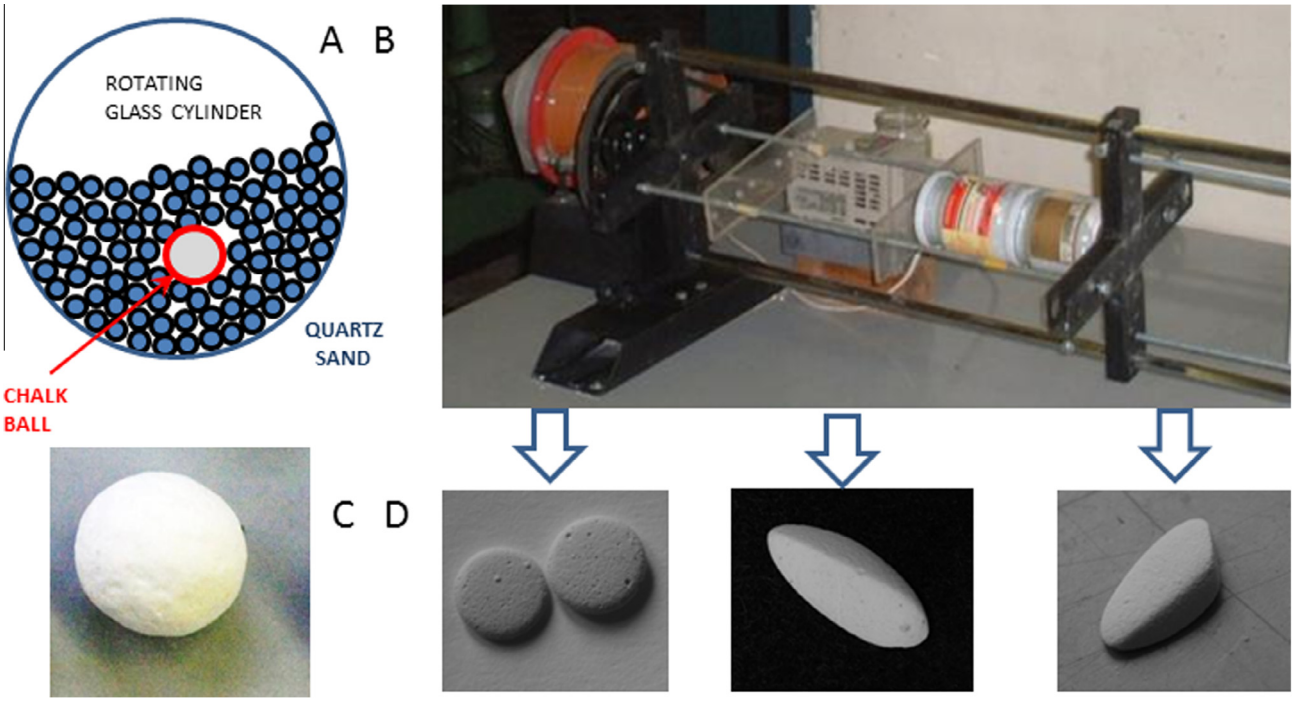

Fig. 8. Scheme (A) and photo (B) of the experimental apparatus; chalk balls before abrasion (C) and three examples of abraded shapes (D) resembling the limit shapes predicted by the abrasion model (Fig. 1).

quantitative modeling of meso-scale surface features suggested that rocks behave more similarly to the Modelled material. Future work will need to be done to resolve this contradiction and to better understand the nature of rock behavior under impact.

A more detailed model of height-dependent intensity would take into account the nonlinear dependence of abrasion intensity on $h(\mathbf{x})$, i.e., the fact that the intensity increases up to a level, and then decreases again. Such a model would predict the beveled surfaces frequently observed on large ventifacts (Bridges et al., 2005).

4. Experiments

The shape of well-worn, mature ventifacts is one of the main hallmarks of ventifact formation under multi-directional winds. The corresponding mathematical model is the isotropic mechanism (defined in the Introduction) and the characteristic mature ventifact shapes appear in this model as *limit shapes,* i.e., geometrical shapes approached in the limit as the volume of the abraded specimen tends towards zero.

In order to verify the model, we compare its limit shapes to shapes created in table-top experiments, much simpler than those of Kuenen (1960). In each of 20 experiments, we rolled 5 rounded chalk pieces of approximately 9.8 mm diameter, surrounded by quartz sand, in a horizontal glass cylinder of diameter 100 mm at 5 rpm for approximately 5 h (Fig. 8). This process can be regarded as an approximation of the isotropic mechanism: as the cylinder turns, both chalk and sand are lifted and dropped periodically, so the chalks pieces suffer large number of micro-collisions with the sand grains, distributed uniformly among all directions. The experimental setup can be regarded as an imitation of aeolian abrasion. Needless to say, our table-top experiment only roughly approximates aeolian abrasion, but it nevertheless appears to give qualitatively correct results. Beyond collisions, abrasion by frictional contact is also a key component of the experiment, which results in a strong bias towards flat limit shapes. Sliding friction between the quartz sand and the abraded chalk particles dominates the process in the time intervals when the chalk remains buried in the sand.

After completing the experiment, we extracted the resulting chalk pieces and found very good qualitative agreement with theoretical predictions of the isotropic mechanism: most pieces could be uniquely identified as being either disk, “Brazil nut,” or tetrahedral (see Fig. 8D for visual comparison). We observed that disk shapes were most frequent among the limit shapes, and tetrahedral shapes also tended to be flat; these features can be attributed to friction. The experiments not only show a good match with natural ventifacts, we also note the good agreement with computer simulations. Compare the last shape in Fig. 4, panel “A” (variable wind) to the Brazil nut shape in Fig. 1 (middle) and Fig. 8D (middle).

5. Discussion, relevance of the results

In this paper we developed and analyzed a partial differential equation – type mathematical model of rock abrasion by sand laden wind. The analysis focused on abrasion under unidirectional wind conditions (“unidirectional mechanism”), as well as abrasion in the presence of multidirectional winds, spanning all spatial directions (“isotropic mechanism”).

In the case of the unidirectional mechanism, our results agree with the established view that the facets and edges of boulders typically reflect one or two dominant wind directions. If complemented with the concept of height-dependent abrasion intensity (Anderson, 1986), our model also shows quantitative agreement with field observations and experimental data (Bridges et al., 2005), predicting that, for immobile clasts, the angles of facets to the horizontal quickly decline until they reach the range ~20–30° (Woodworth, 1894; Schoewe, 1932), after which the rate of change becomes extremely slow (Bryan, 1931; Kuenen, 1928; King, 1936. Unidirectional abrasion appears also in other geological scenarios. For example, the evolution of bedrock profiles under repeated impacts with bedload can be accurately modeled by this mechanism (Sipos et al., 2010; Domokos et al., 2014.) Here, unlike

in the case of ventifacts, the abradant size cannot be neglected and the underlying mathematical models are more complex (Bloore, 1977; Várkonyi and Domokos, 2011).

The isotropic mechanism is unrealistic in terms of a wind regime, but is a reasonable model of the abrasion of a small specimen, which is frequently overturned. Under these conditions, whenever the orientation of a rock changes, another side of the rock is attacked by the wind. As discussed earlier, the isotropic mechanism transforms any initial shape to one of three 'ultimate' shapes, two of which resemble the most common mature ventifact morphologies: pyramidal dreikanters and triquetrous Brazil nut shapes (Fig. 1). This coincidence of form is our primary evidence that this mechanism may have significant role in shaping small ventifacts. The isotropic mechanism is also present at a larger scale: the formation of flat areas and sharp edges on asteroids was recently explained by micrometeorite collisions with the aid of the same abrasion model (Domokos et al., 2009).

Our modeling framework can also handle other probability distributions of wind directions, but such an extension of our investigations is beyond the scope of the paper. We just briefly mention one relevant example: in the presence of two dominant and opposing wind directions, the model predicts two facets meeting at a sharp keel, as observed in field conditions.

By analyzing predictions of the model, we have identified two distinct mechanisms responsible for the facets and sharp edges of ventifacts. The most efficient, which we refer to as a "unidirectional mechanism," operates on immobile clasts, in the presence of one or a few dominant wind directions, and it exploits the brittle behavior of the rock material. The role of this mechanism in facet formation has been recognized by many earlier works, but our model is the first one to combine wind characteristics and material abrasion susceptibility into a quantitative description of the morpho-evolution of abrading rocks. We have also identified a second mechanism, referred to as "isotropic mechanism," that operates on small ventifacts, which are frequently overturned during the abrasion process. This is somewhat less efficient than the unidirectional mechanism, but its effect does not depend on material behavior (brittle or ductile) or wind characteristics (the presence of dominant directions). The modeled isotropic mechanism developed a small set of mature ventifact shapes, which shows agreement with field observations.

This paper is significant in that it addresses long-standing questions (Travers, 1870; Woodworth, 1894; Schoewe, 1932; Needham, 1937; Kuenen, 1960; Greeley et al., 1982; Anderson, 1986; Bridges et al., 2004) as to facet formation and the morphological evolution of faceted ventifacts. Our results agree with both qualitative (mature shapes of small ventifacts, orientation of facets relative to the wind on large ventifacts) and quantitative (decay of facet angles) observations. Furthermore, the numerical modeling ties in with earlier experimental work on the role of material type (Greeley et al., 1982). The modeling helps us to visualize geomorphic developments that cannot be observed directly in the field owing to scale and time constraints. Ultimately, our understanding of the formation of ventifacts enables us to ascertain their value as criteria of past climatic conditions on Earth and Mars and enhance our understanding of past wind directions and types of wind systems.

Acknowledgements

Péter L. Várkonyi and Gábor Domokos have been supported by the National Research, Development and Innovation Office, Hungary under grant 104601. The authors thank Ottó Sebestyén for his invaluable help with the experiments. Julie E. Laity has received support from internal grants at California State University, Northridge.

References

Anderson, R.S., 1986. Erosion profiles due to particles entrained by wind: application of an eolian sediment-transport model. Geol. Soc. Am. Bull. 97, 1270–1278.
Anderson, R.S., Anderson, S.P., 2010. Geomorphology: The Mechanics and Chemistry of Landscapes. Cambridge University Press.
Barchyn, T.E., Hugenholtz, C.H., 2015. Yardang evolution from maturity to demise. Geophys. Res. Lett. 42, 5865–5871.
Bather, F.A., 1900. Wind-worn pebbles in the British Isles. Proc. Geol. Assoc. 16, 396–420.
Blake, W.P., 1855. On the grooving and polishing of hard rocks and minerals by dry sand. Am. J. Sci. 20, 178–181.
Bourke, M.C., Viles, H. (Eds.), 2007. A Photographic Atlas of Rock Breakdown Features in Geomorphic Environments. Planetary Science Institute, Tucson, Arizona, USA.
Bloore, F.J., 1977. The shape of pebbles. Math. Geol. 9, 113–122.
Bridges, N.T., Greeley, R., Haldemann, A.F.C., Herkenhoff, K.E., Kraft, M., Parker, T.J., Ward, A.W., 1999. In: Ventifacts at the pathfinder landing site. J. Geophys. Res.: Planets 104 (E4), 8595–8615 (1991–2012).
Bridges, N.T., Laity, J.E., Greeley, R., Phoreman, J., Eddlemon, E.E., 2004. Insights on rock abrasion and ventifact formation from laboratory and field analog studies with applications to Mars. Planet. Space Sci. 52, 199–213.
Bridges, N.T., Phoreman, J., White, B.R., Greeley, R., Eddlemon, E., Wilson, G., Meyer, C., 2005. Trajectories and energy transfer of saltating particles onto rock surfaces: application to abrasion and ventifact formation on Earth and Mars. J. Geophys. Res. 110, E12.
Bridges, N.T., Calef, F.J., Hallet, B., Herkenhoff, K.E., Lanza, N.L., Le Mouélic, S., Newman, C.E., Blaney, D.L, de Pablo, Kocurek, G.A., Langevin, Y., Lewis, K.W., Mangold, N., Maurice, S., Meslin, P.-Y., Pinet, P., Renno, N.O., Rice, M.S., Richardson, M.E., Sautter, V., Sletten, R.S., Wiens, R.C., Yingst, R.A., 2014. The rock abrasion record at gale crater: Mars science laboratory results from bradbury landing to rocknest. J. Geophys. Res.: Planets 119 (6), 1374–1389. http://dx.doi.org/10.1002/2013JE004579.
Bryan, K., 1931. Wind-Worn Stones or Ventifacts–A Discussion and Bibliography, 98. National Research Council Circular, Washington, DC, p. 1929–1930.
Cooke, R.U., Warren, A., Goudie, A., 1993. Desert Geomorphology. Taylor & Francis.
Domokos, G., Sipos, A.Á., Szabó, G., Várkonyi, P.L., 2009. Formation of sharp edges and planar areas of asteroids by polyhedral abrasion. Astrophys. J. 699, L13.
Domokos, G., Gibbons, G.W., Sipos, A.Á., 2014. Circular, stationary profiles emerging in unidirectional abrasion. Math. Geosci. 46, 483–491.
Enys, J.D., 1878. On sand-worn stones from New Zealand. Q. J. Geol. Soc. 34, 86–88.
Finnie, I., 1995. Some reflections on the past and future of erosion. Wear 186, 1–10.
Gillies, J.A., Nickling, W.G., Tilson, M., 2009. Ventifacts and wind-abraded rock features in the Taylor Valley, Antarctica. Geomorphology 107, 149–160.
Greeley, R., Leach, R.N., Williams, S.H., White, B.R., Pollack, J.B., Krinsley, D.H., Marshall, J.R., 1982. Rate of wind abrasion on Mars. J. Geophys. Res.: Solid Earth 87, 10009–10024.
Greeley, R., Williams, S.H., White, B.R., Pollack, J.B., Marshall, J.R., 1985. Wind abrasion on Earth and Mars. In: Woldenberg, M.J. (Ed.), Models in Geomorphology, 373–422.
Greeley, R., Bridges, N.T., Kuzmin, R.O., Laity, J.E., 2002. Terrestrial analogs to wind-related features at the viking and pathfinder landing sites on Mars. J. Geophy. Res.: Planets 107, 5.1–5.21.
Hazewinkel, M. (Ed.), 2001. Gauss-Bonnet Theorem, Encyclopedia of Mathematics. Springer, URL: <http://www.encyclopediaofmath.org/index.php/Gauss-Bonnet_theorem>.
Hoare, P.G., Stevenson, C.R., Godby, S.P., 2002. Sand sheets and ventifacts: the legacy of aeolian action in west Norfolk, UK. Proc. Geolo. Assoc. 113, 301–317.
King, L.C., 1936. Wind-Faceted Stones from Maryborough, New Zealand. J. Geol. 44, 201–213.
Knight, J., 2003. Note on the formation of ventifacts at Castlerock, Northern Ireland coast. Irish J. Earth Sci. 21, 39–45.
Knight, J., 2008. The environmental significance of ventifacts: a critical review. Earth Sci. Rev. 86, 89–105.
Knight, J., Burningham, H., 2003. Recent ventifact development on the central Oregon coast, western USA. Earth Surf. Proc. Land. 28, 87–98.
Kuenen, P.H., 1928. Experiments on the formation of wind-worn pebbles. Leidsche Geol. Med. 3, 17–38.
Kuenen, P.H., 1960. Experimental abrasion 4: eolian action. J. Geol. 68, 427–449.
Laity, J.E., 1987. Topographic effects on ventifact development, Mojave Desert, California. Phys. Geogr. 8, 113–132.
Laity, J.E., 2009. Landforms, Landscapes, and Processes of Aeolian Erosion, .. In: Parsons, A.J., Abrahams, A.D. (Eds.), Geomorphology of Desert Environments, second ed. Springer Science þ Business Media B.V., p. 597–627.
Laity, J.E., Bridges, N.T., 2009. Ventifacts on Earth and Mars: analytical, field, and laboratory studies supporting sand abrasion and windward feature development. Geomorphology 105, 202–217.
Malin, M.C., 1988. Abrasion in ice-free areas of southern Victoria Land, Antarctica. Ant. J. US (Review 22), 38–39.

Miotke, F.D., 1982. Formation and rate of formation of ventifacts in Victoria Land, Antarctica. Polar Geogr. 6, 98–113.
Mitchell, I.M., 2008. The flexible, extensible and efficient toolbox of level set methods. J. Sci. Comput., 300–329
Needham, C.E., 1937. Ventifacts from New Mexico. J. Sediment. Res. 7, 31–33.
Schoewe, W.H., 1932. Experiments on the formation of wind-faceted pebbles. Am. J. Sci. 140, 111–134.
Selby, M.J., 1977. Palaeowind directions in the central Namib Desert, as indicated by ventifacts. Modoqua 10, 195–198.
Sharp, R.P., 1949. Pleistocene ventifacts east of the big horn mountains, Wyoming. J. Geol. 57, 175–195.
Sharp, R.P., 1980. Wind-driven sand in Coachella Valley, California: further data. Geol. Soc. Am. Bull. 91, 724–730.
Sipos, A.Á., Domokos, G., Wilson, A., Hovious, N., 2010. A discrete random model describing bedrock profile abrasion. Math. Geosci. 43, 583–591.
Stone, G.H., 1886. Wind action in Maine. Am. J. Sci. 182, 133–138.
Sugden, W., 1964. Origin of faceted pebbles in some recent desert sediments of southern Iraq. Sedimentology 3, 65–74.
Thomson, B.J., Bridges, N.T., Greeley, R., 2008. Rock abrasion features in the Columbia Hills, Mars. J. Geophys. Res. 113. http://dx.doi.org/10.1029/2007JE003018.
Travers, W.T.L., 1870. On the sandworn stones of Evan's Bay. Transactions of the New Zealand Institute 2, 247–248.
Várkonyi, P.L., Domokos, G., 2011. A general model for collision-based abrasion processes. IMA J. Appl. Math. 76, 47–56.
Várkonyi, P.L., Laity, J.E., 2012. Formation of surface features on ventifacts: Modeling the role of sand grains rebounding within cavities. Geomorphology 139, 220–229.
Wade, A., 1910. On the formation of dreikante in desert regions. Geol. Mag. 7, 394–398.
Wang, Z.T., Wang, H.T., Niu, Q.H., Dong, Z.B., Wang, T., 2011. Abrasion of yardangs. Phys. Rev. E 84, 031304.
Wentworth, C.K., Dickey, R.I., 1935. Ventifact localities in the United States. J. Geol., 97–104
Woodworth, J.B., 1894. Postglacial eolian action in southern New England. Am. J. Sci. 277, 63–71.